Multicritical behavior of the antiferromagnetic spin-3/2 Blume-Capel model: Finite-size-scaling and Monte Carlo studies

Smaîne Bekhechi
Laboratoire de Magnétisme et Hautes Energies, Département de Physique, Faculté des Sciences, Boîte Postale 1014, Rabat, Morocco
and Laboratoire de Physique Théorique, Département de Physique, Faculté des Sciences, Boîte Postale 1014, Rabat, Morocco

Abdelilah Benyoussef
Laboratoire de Magnétisme et Hautes Energies, Département de Physique, Faculté des Sciences, Boîte Postale 1014, Rabat, Morocco
(Received 21 June 1996; revised manuscript received 15 July 1997)

Transfer-matrix finite-size-scaling calculations and Monte Carlo simulations are used to investigate the two-dimensional spin-3/2 Ising antiferromagnet in the presence of an external magnetic field and a single-ion potential. Comparison is made between the results of this study and previous mean-field calculations. The phase diagrams and the critical behavior of the model are discussed. In contrast to the mean-field picture, no decomposition of the tricritical point is observed.
[S0163-1829(97)00845-X]

I. INTRODUCTION

Spin-3/2 models have been introduced earlier to explain phase transition[1] in $DyVO_4$ (Refs. 2,3) and tricritical properties in ternary fluid mixtures.[4] They have been studied by mean-field approximation (MFA). Recently the phase transition in the spin-3/2 Blume-Emery-Griffith (BEG) model with nearest-neighbor interaction, both bilinear and biquadratic, and with a crystal-field interaction has been studied within the MFA and Monte Carlo simulation[5] and by the renormalization-group method.[6]

Transfer-matrix methods and Monte Carlo simulations applied to finite systems and finite-size-scaling theory have been used with great success to study the critical properties of Ising models.[7–11] In the case of the spin-1 Ising antiferromagnetic Blume-Capel model[12,13] in the presence of an external magnetic field in two dimensions, they have shown that there is no decomposition of the tricritical line into a line of critical end points and one of double critical points.[14,15] This decomposition has been found by MFA (Ref. 16) and confirmed by Monte Carlo simulation on a three-dimensional cubic lattice.[17]

Using the mean-field approximation, the multicritical behavior of the spin-3/2 Blume-Capel model with antiferromagnetic bilinear interaction, with a crystal field and under an external magnetic field, has been investigated.[18] The results reconfirm the decomposition of the tricritical point for this higher spin order model. Earlier, Motizuki[19] performed mean-field calculations for the spin-1/2 Ising model with antiferromagnetic nearest-neighbor and ferromagnetic next-nearest-neighbor exchange interactions and found that below a given ratio R of the intrasublattice to intersublattice coupling the decomposition also holds for this model. However, Monte Carlo renormalization-group study[20] yielded results which were inconsistent with the mean-field picture and recent Monte Carlo simulation[21] exclude the decomposition of the tricritical point even for small R in three dimensions for this model. Mean-field approximation predicts also for other models the existence of multicritical points, such as the $S=1/2$ Ising model in a random field obeying a symmetric three-peak distribution[22] and the spin-1 BEG model with repulsive biquadratic coupling.[23]

In this paper we realize a thorough investigation of a two-dimensional antiferromagnetic spin-3/2 Blume-Capel model in an external magnetic field by using transfer-matrix finite-size-scaling (TMFSS) calculations and Monte Carlo simulations. An approach which includes the correlated fluctuations ignored by the mean-field approximation. The objectives of this study are (i) to confirm, for $H=0$, the existence of the end point instead of a tricritical point,[5] (ii) to determine the global phase diagram in the T-H-D parameter space, (iii) to investigate whether the tricritical point decomposes into a bicritical point and a critical end point as predicted by mean-field approximation.

The model studied in this paper is defined by the Hamiltonian:

$$\mathcal{H}=-J\sum_{\langle ij\rangle} S_iS_j+D\sum_i S_i^2-H\sum_i S_i. \qquad (1)$$

Here the spin variables are localized on sites of a square lattice with periodic boundary conditions and take the values $\pm 3/2$ and $\pm 1/2$. The first term describes the antiferromagnetic coupling ($J<0$) between the spins at sites i and j, this interaction is restricted to the z nearest-neighbor pairs of spins. The second term describes the single-ion anisotropy and the last term represents the effect of an external magnetic field. The Hamiltonian and the phase diagrams are invariants under the transformation ($H\rightarrow -H, S\rightarrow -S$).

The remainder of this paper is organized as follows: In Sec. II, we briefly outline the formalism of the transfer-matrix finite-size-scaling method and the Monte Carlo method is described in Sec. III. In Sec. IV, our numerical results are presented and Sec. V contains a summary and a conclusion.

II. TRANSFER-MATRIX FINITE-SIZE-SCALING CALCULATIONS

Detailed description of the phenomenological finite-size-scaling method and transfer-matrix formalism on two-dimensional systems are given in Refs. 24,25. A system of linear size N is used with periodic boundary conditions and only even values of N are considered to avoid the introduction of interfaces and to preserve the antiferromagnetic phase. With $N'=N+2$ the Nightingale condition[24] for the determination of the critical point K_c becomes

$$\frac{\xi_N(K_c)}{N}=\frac{\xi_{N+2}(K_c)}{N+2}, \tag{2}$$

where $\xi_N(K)$ is the correlation length. The symbol K denotes the set of fields $K=(T,D,H)$. Determining whether the transition is first-order or continuous is accomplished by examining the finite-size-scaling behavior of the persistence length $\tilde{\xi}$.[8,15,26] If the scaled persistence length $\tilde{\xi}/N$ on the transition line is a decreasing function of N then the transition is continuous, otherwise the transition is first order.

The correlation length and persistence length are obtained from the three largest eigenvalues of the transfer matrix. In the transfer-matrix (TM) method, the lattice is approximated by an $N\times\infty$ lattice with periodic boundary conditions in the finite direction. The full $4^N\times 4^N$ transfer matrix was block diagonalized utilizing invariance under one step translations in the transverse direction. The symmetric and the antisymmetric blocks, T^S (700×700 for $N=6$) and T^A (696×696 for $N=6$), are the only two blocks whose symmetries correspond to the ordered phases. We diagonalized them with the RS library routines (based on EISPACK routines) on DEC station 5000/200. The diagonalization results in three eigenvalues of interest. The largest eigenvalue of both T^S and the transfer matrix is λ_1^s. By virtue of the Perron-Frobenius theorem, it is positive and nondegenerate. The other two eigenvalues are λ_2^s, second largest of T^S, and λ_1^A, the largest eigenvalue of T^A. The correlation and the persistence lengths are, respectively, given by

$$\xi_1^A=(\ln|\lambda_1^s/\lambda_1^A|)^{-1},$$
$$\xi_1^s=(\ln|\lambda_1^s/\lambda_2^s|)^{-1}. \tag{3}$$

The correlation length exponent ν is obtained following the argument of Nightingale[24] where a field differentiation is used, while the exponent η for the decay of the correlation function is determined by using the conjecture, due to Derrida and de Seze,[27] or by using an argument based on conformal invariance.[28] These arguments predict that

$$\eta_N=N/[\pi\xi_1^A(N)]. \tag{4}$$

Since for $N=2$ the estimates of the critical temperature and the exponents are not very accurate and for $N=8$ an entire block (of about 8230) of the transfer matrix could not be stored in the available computers, so we find it reasonable to stop here and no extrapolation of the results is performed.

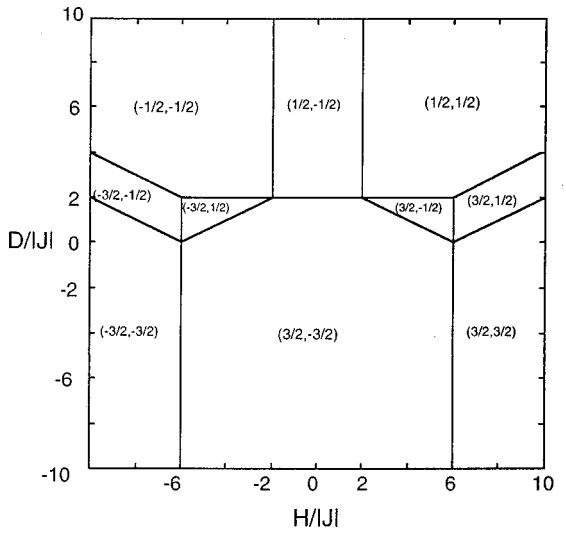

FIG. 1. Ground-state phase diagram.

III. MONTE CARLO SIMULATION

We have performed Monte Carlo simulation to complement TMFSS calculations. The system studied is an $L\times L$ square lattice with even L, containing $N=L^2$ spins, and we use the well-known Metropolis algorithm[29] with periodic boundary conditions to update the lattice configurations. The physical quantity of use is the staggered magnetization $(J<0)|M|$ and is estimated by

$$|M|\equiv\langle|M_s|\rangle=\frac{1}{NS}\sum_c\sum_i\delta_i S_i(c), \tag{5}$$

where i runs over the lattice sites and $\delta_i=+1(\delta_i=-1)$ for sites on the even (odd) sublattice, respectively. c runs over the configurations obtained to update the lattice over one sweep of the entire N spins of the lattice (one Monte Carlo step, MCS), counted after the system reaches thermal equilibrium, and S is the number of the MCS.

In order to measure the phase boundaries we shall find useful the measurement of fluctuations (variance of the order-parameter) in M_s defined by the staggered magnetic susceptibility:

$$\chi_m=\frac{N}{kT}(\langle M_s^2\rangle-\langle|M_s|\rangle^2). \tag{6}$$

IV. RESULTS AND DISCUSSION

A. Phase diagrams

In order to calculate the ground-state energy, we divide the lattice into two equivalent sublattices a and b and express the Hamiltonian as a sum of the contributions of the pairs of nearest neighbors. By comparing the values of the different configurations, we obtain the ground-state phase diagram Fig. 1.

For $H/|J|\geq0$, there are four ordered ground states, a ferrimagnetic (3/2,1/2) an antiferrimagnetic (3/2,−1/2) state, and two with antiferromagnetic symmetry. Referring to the sublattice magnetization (M_a,M_b), we denote these states

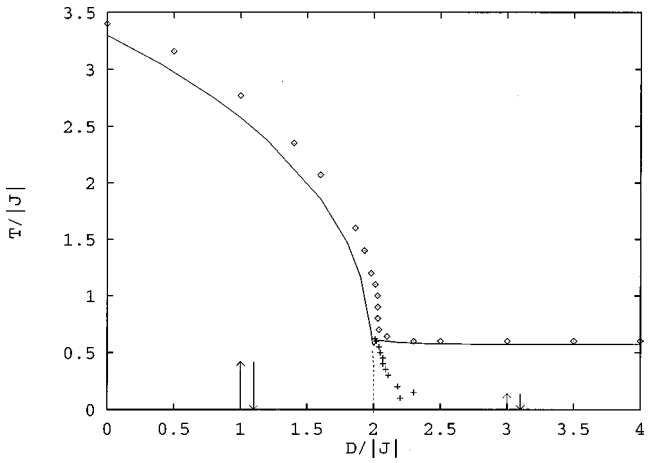

FIG. 2. Phase diagram for $H/|J|=0$ as obtained by TMFSS calculations with $N'/N=4/6$. Solid line represents critical points and dashed line is the first-order transition. Monte Carlo results are also included for $L=30$. ◇ represents critical points and + indicates first-order transitions.

by (3/2,−3/2), (1/2,−1/2), respectively. When $H/|J|$ becomes strong we have two uniform ground states termed as (3/2,3/2) and (1/2,1/2).

For $T\neq 0$, most of the phase diagrams in the $(D/|J|,H/|J|,T/|J|)$ space are obtained by transfer-matrix finite-size-scaling calculations with $N'/N=4/6$. Most of the Monte Carlo data are obtained with lattices of size $L=30$ and some results with $L=40$ and 60.

(i) In the absence of the external magnetic field, $H/|J|=0$, the behavior of the antiferromagnet, Fig. 2, is similar to the ferromagnet. There is a second-order transition line separating the disordered phase from the two antiferromagnetic phases (3/2,−3/2) and (1/2,−1/2) which are separated by a first-order line. This line terminates at an end point at $(D/|J|=1.99\pm 0.01;\ T/|J|=0.513\pm 0.001)$. To locate the first-order line and the end point, the behavior of the persistence length in the $D/|J|$ direction is used. In this case, the persistence length has a sharp peak, increasing as e^N, at the first-order transition. As one crosses the first-order transition close to the critical point, $\xi_1^s(6)$ peaks much less sharply than at lower temperature. At the point where $\xi_1^s(6)/6=\xi_1^s(4)/4$ become tangent at their peaks rather than below T_c, we interpret that the Nightingale criterion is being satisfied at the critical edge of the first-order line.[30] On the other hand, we have also performed Monte Carlo simulations for $H/|J|=0$. The data were obtained for a lattice of size $L=30$ and 10 000 MCS after 5000 sweeps had been discarded for thermal equilibrium. The phase diagram is similar to that obtained by TMFSS calculations. The second-order phase boundary was obtained from peaks in the magnetic susceptibility. Along the first-order line strong hysteresis was observed when crossing this line in the $D/|J|$ direction. The critical point was determined when the hysteresis disappears, it occurs at $(D/|J|=2.01\pm 0.01;\ T/|J|=0.62\pm 0.01)$, Figs. 3(a)–3(c). We locate the first-order line by using the mixed start technique[11] in which the upper half of the lattice was initialized to the $T=0$ configuration expected on one side of the first-order boundary (3/2,−3/2), and the lower half plane initialized to the configuration expected on the other side of

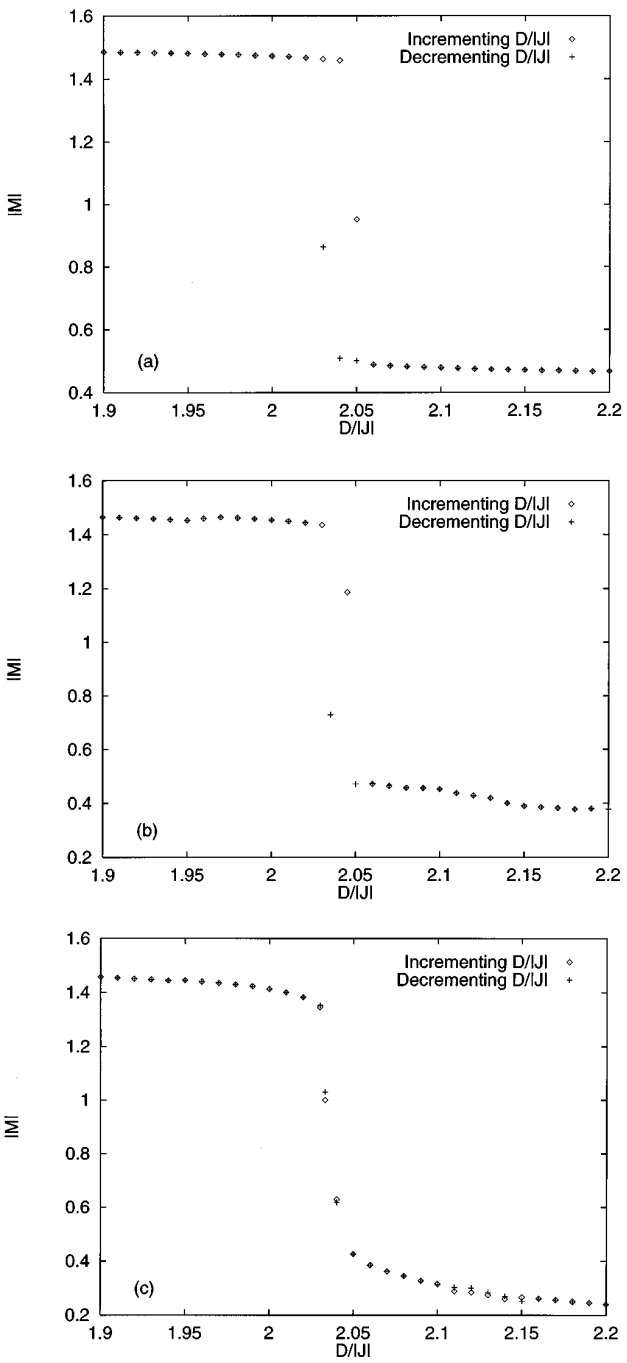

FIG. 3. Typical hysteresis observed when crossing the first-order transition boundary for $H/|J|=0$, and with $L=30$, MCS $=10\,000$. (a) $T/|J|=0.5$, (b) $T/|J|=0.55$, (c) $T/|J|=0.62$.

the first order boundary (1/2,−1/2). By using this technique we were able to locate the first-order transition. The differences are explained by the fact that MC simulation overestimates the critical temperature, while the TM method underestimates it. So by increasing the system size the critical temperature obtained by MC calculations decrease and TM results increase in such a way that by using finite-size-scaling extrapolation of the results, these differences could be eliminated as discussed in Ref. 15. Our results obtained by these two methods reconfirm our previous study[18] of the existence of the end point instead of the tricritical point found by Barreto *et al.* in the ferromagnetic case.[5]

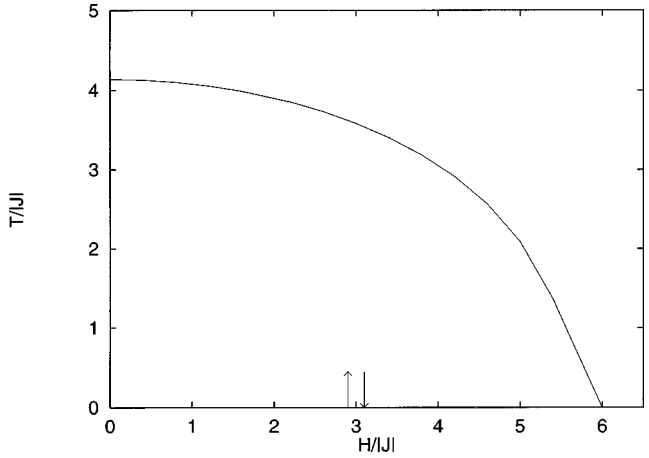

FIG. 4. Phase diagram for $D/|J|=-2$ based on TMFSS calculations with $N'/N=4/6$. Solid line represents critical points.

(ii) In the presence of the magnetic field, $H\neq 0$, the behavior of the antiferromagnet is completly different from the ferromagnet. For negative values of $D/|J|$, $D/|J|<0$, the transition line between the antiferromagnetic phase (3/2, $-3/2$) and the disordered phase is always of second order, Fig. 4.

For $0\leqslant D/|J|<1.99$, Fig. 5, the disordered phase is separated from the antiferromagnetic $(3/2,-3/2)$, the antiferrimagnetic $(3/2,-1/2)$, and the ferrimagnetic (3/2,1/2) phases by a line of critical points.

As $D/|J|$ is increased, $D/|J|\geqslant 2$, the phase diagram is divided into two blocks of critical points, separating the disordered phase from the ferrimagnetic phase, (3/2,1/2) and the antiferromagnetic phase, $(1/2,-1/2)$, at high and low magnetic field, respectively, Figs. 6(a) and 6(b).

B. Nondecomposition of the tricritical point

One of the most interesting and elusive features, predicted by mean-field theory, is the decomposition of the tricritical point into a critical end point and a double critical point.[18] To confirm or not this issue, we have investigated the phase diagram in the region where the nature of the phase transition changes, in the neighborhood of $D/|J|\approx 2$. We have

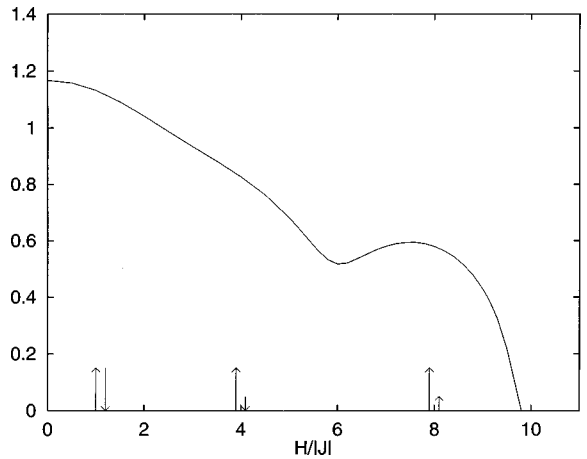

FIG. 5. Phase diagram for $D/|J|=1.9$ based on TMFSS calculations with $N'/N=4/6$. Solid line represents critical points.

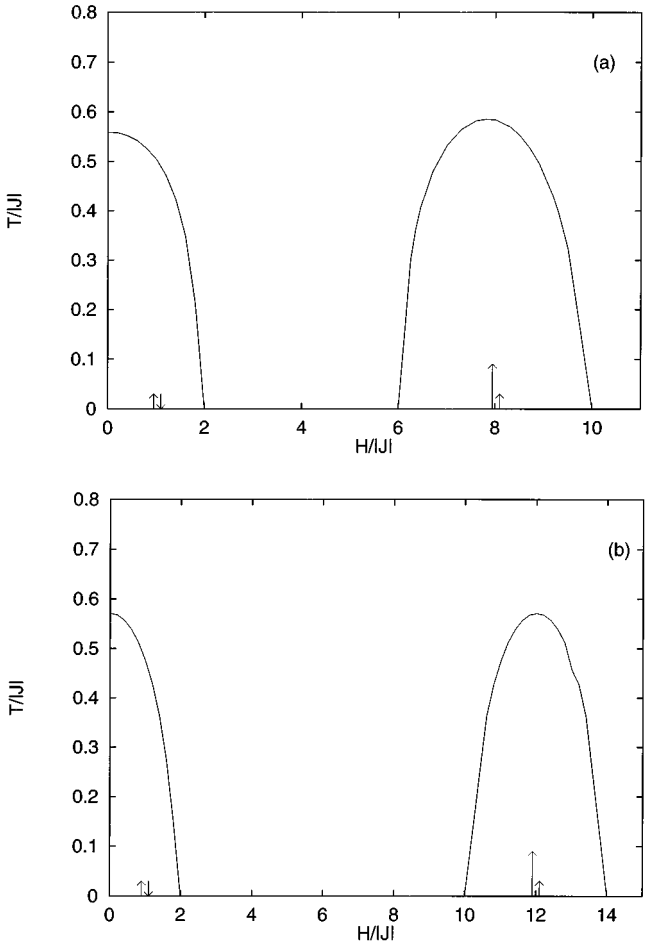

FIG. 6. Phase diagram for $D/|J|\geqslant 2$ based on TMFSS calculations with $N'/N=4/6$. Solid line represents critical points. (a) $D/|J|=2$, (b) $D/|J|=4$.

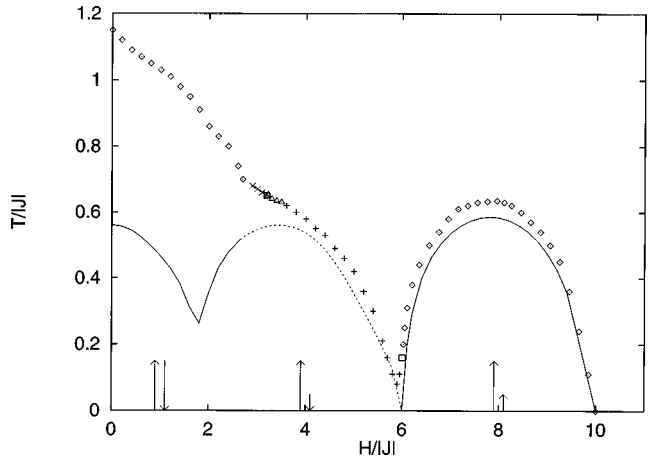

FIG. 7. Phase diagram for $D/|J|=1.992$ where decomposition would be expected based on TMFSS calculations with $N'/N=4/6$. Solid line represents critical points and dashed line is the first-order transition. A tricritical point occurs. Monte Carlo results are also included for $L=30$. $\diamond$ denotes critical points and $+$ denotes first-order transitions. In the neighborhood of the tricritical point, simulations for $L=40$ are added, where $\times$ represents critical points and $\triangle$ denotes first-order transitions. Two tricritical points denoted by $\boxdot$ occur.

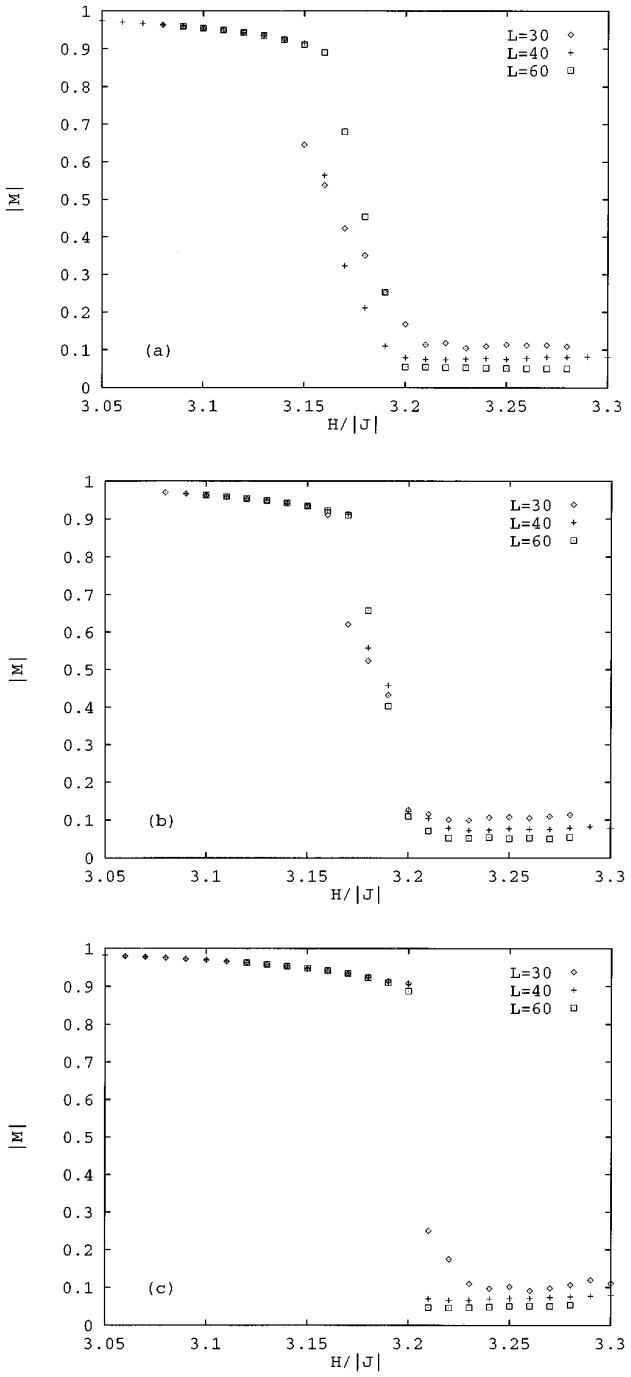

FIG. 8. Comparaison of the phase transition for $L=30$, 40, and 60 at (a) $T/|J|=0.66$, $H_c/|J|\approx 3.18$ where a continuity in the order parameter occurs which is characteristic of a second-order transition, (b) $T/|J|=0.65$, $H_c/|J|\approx 3.2$ which shows a behavior between first- and second-order transitions, with that at (c) $T/|J|=0.64$, $H_c/|J|\approx 3.22$, which shows the discontinuity indicative of a first-order phase transition.

performed transfer-matrix finite-size-scaling calculations at $D/|J|=1.992$ with $N'/N=4/6$, Fig. 7. In this figure, the disordered phase is separated from the ordered phases, (3/2, $-3/2$) and (3/2,1/2), by a line of critical points at low and high magnetic field, respectively. For $2.65\leqslant H/|J|\leqslant 6$, the disordered phase is separated from the antiferrimagnetic phase (3/2,$-1/2$) by a line of first-order transition. This line

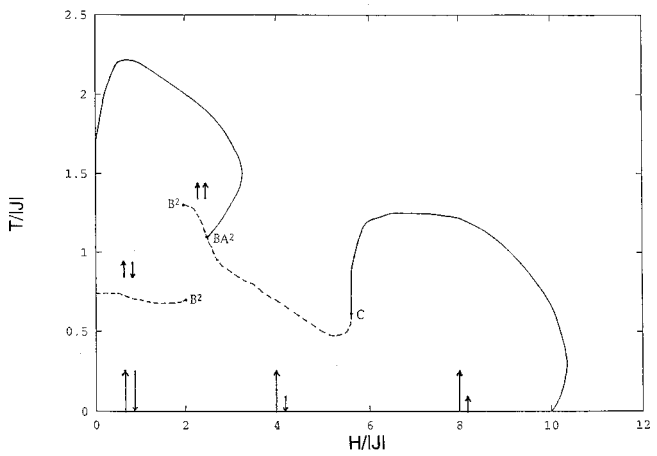

FIG. 9. Mean-field calculation for $D/|J|=1.98$ from Ref. 18. Solid lines represent second-order transitions and dashed lines represent first-order transitions. B^2 and BA^2 design the double critical point and the critical point, respectively.

meets the continuous line at a tricritical point, $H_t/|J|=2.65\pm 0.01$ and $T_t/|J|=0.516\pm 0.001$, as determined from the persistence length. We have also realized Monte Carlo simulations for the same value of $D/|J|=1.992$. The general shape of the phase diagram is the same as that determined by TMFSS. For $H/|J|<3.2$ and $H/|J|>6.0$, there is a continuous transition separating the disordered phase from the ordred phases. The points of this boundary were determined by observation of peaks in the staggered magnetic susceptibility. For $3.2\leqslant H/|J|\leqslant 6.0$, the phase boundary is distinctly first order. In this region of H the first-order phase boundary exhibited a decided discontinuity in $|M|$ as well as the hysteresis one would expect of a first-order phase transition. In the region where the decomposition is expected, we have made high statistics measurements for lattices of size $L=30$, 40, 60, and the length of the simulation varied from $S=100\,000$ to 250 000. The location of the tricritical point was determined by using the observation of the beginning of the discontinuity in the order parameter $|M|$ as the boundary of the first-order region is encountered from the second-order side, Figs. 8(a)–8(c). Our estimate of the tricritical point values are $(H_t/|J|)_1=3.2\pm 0.02$, $(T_t/|J|)_1=0.65\pm 0.01$ and $(H_t/|J|)_2=6.0\pm 0.02$, $(T_t/|J|)_2=0.16\pm 0.04$. The main differences are due to strong finite-size effects at low magnetic field in Monte Carlo simulations and the small sizes used here for the transfer-matrix calculations which does not give the second tricritical point at high magnetic field as determined from the mean-field calculations, Fig. 9.

To confirm this nondecomposition we have also calculated the exponents ν and η for $N/N'=4/6$. In order to have better values for ν, both on the critical surface and along the tricritical line, we have performed field differentiation (in the D direction). Along the critical line, far from the regions $D/|J|=2.0$ and $D/|J|=6.0$ where finite-size effects are strong, we find $\nu=0.9644$ and $\eta=0.2517$ which are both in good agreement with the expected values of the two-dimensional Ising critical values, $\nu=1$ and $\eta=1/4$.[31,32] At the tricritical point, we find $\nu_t=0.5451$ and $\eta_t=0.1401$, which are also in good agreement with the two-dimensional Ising tricritical values, $\nu_t=5/9$ and $\eta_t=3/20$.[33,34] These results re-

confirm that the first- and the second-order surfaces join smoothly together at the tricritical line.

V. SUMMARY AND CONCLUSION

We have made a detailed TMFSS calculations and Monte Carlo study of the phase diagram in the $(D/|J|, H/|J|, T/|J|)$ space and criticality of the antiferromagnetic Blume-Capel spin-3/2 model on a two-dimensional lattice. We have confirmed our previous study[18] for the existence of the end point for $H/|J|=0$ instead of the tricritical point.[5] We have also studied the question of the decomposition of the tricritical point for $H \neq 0$. No evidence is found for such a decomposition. This nondecomposition is confirmed by our estimates for the exponent η and ν, which are in good agreement with those of the two-dimensional Ising model. In order to compare these results with previous work, we show in Fig. 9 the prediction of the mean-field calculations.[18] In particular, Fig. 9 shows the decomposition of the tricritical point into a critical end point BA^2 and a double critical point B^2. This disagreement between mean-field calculations and the present results is readily explained. In the mean-field calculations correlated fluctuations are neglected, while for the two-dimensional lattice, fluctuations are strong in TMFSS calculations and Monte Carlo simulations and they break down the first-order phase transition associated with the decomposition. Since the critical dimensionality for tricritical systems is $d=3$ where the mean-field picture would be correct, it is important to investigate this model by Monte Carlo simulation in $d=3$ using the histogram and Monte Carlo renormalization-group method to determine the exponents. This is a question which we leave for further study.

ACKNOWLEDGMENT

S.B. thanks the International Centre for Theoretical Physics of Trieste (I.C.T.P) for financial support.

[1] J. Sivardière and M. Blume, Phys. Rev. B **5**, 1126 (1972).
[2] A. H. Cooke, D. M. Martin, and M. R. Wells, J. Phys. (Paris), Colloq. **32**, C1-488 (1971).
[3] A. H. Cooke, D. M. Martin, and M. R. Wells, Solid State Commun. **9**, 519 (1971).
[4] S. Krinsky and D. Mukamel, Phys. Rev. B **11**, 399 (1975).
[5] F. C. Barreto and O. F. de Alcantara Bonfim, Physica A **172**, 378 (1991).
[6] A. Bakchich, A. Bassir, and A. Benyoussef, Physica A **195**, 188 (1993).
[7] P. A. Rikvold, K. Kaski, J. D. Gunton, and M. C. Yalabik, Phys. Rev. B **29**, 6285 (1984), and references therein.
[8] P. D. Beale, Phys. Rev. B **33**, 1717 (1986).
[9] W. Kinzel and M. Schick, Phys. Rev. B **23**, 3435 (1981).
[10] N. C. Bartelt, T. L. Einstein, and L. D. Roelofs, Phys. Rev. B **34**, 1616 (1986); L. D. Roelofs, T. L. Einstein, N. C. Bartelt, and J. D. Shore, Surf. Sci. **176**, 295 (1986).
[11] K. Binder, *Application of the Monte Carlo methods in statistical physics* (Springer-Verlag, Berlin, 1994), and references therein.
[12] M. Blume, Phys. Rev. **141**, 517 (1966).
[13] H. W. Capel, Physica (Amsterdam) **32**, 966 (1966); **33**, 295 (1967).
[14] J. D. Kimel, S. Black, P. Carter, and Y. L. Wang, Phys. Rev. B **35**, 3347 (1987).
[15] J. D. Kimel, P. A. Rikvold, and Y. L. Wang, Phys. Rev. B **45**, 7237 (1992).
[16] Y. L. Wang and K. Rauchwarger, Phys. Lett. **59A**, 73 (1976).
[17] Y. L. Wang and J. D. Kimel, J. Appl. Phys. **69**, 6176 (1991).
[18] A. Bakchich, S. Bekhechi, and A. Benyoussef, Physica A **210**, 415 (1994).
[19] K. Motizuki, J. Phys. Soc. Jpn. **14**, 759 (1959).
[20] H. J. Herrmann, E. B Rasmussen, and D. P. Landau, J. Appl. Phys. **53**, 7994 (1982).
[21] H. J. Herrmann and D. P. Landau, Phys. Rev. B **48**, 239 (1993).
[22] M. Kaufman, P. E. Klunzinger, and A. Khurana, Phys. Rev. B **34**, 4766 (1986).
[23] W. Hoston and A. N. Berker, Phys. Rev. Lett. **67**, 1027 (1991).
[24] M. P. Nightingale, Physica A **83**, 561 (1976); Phys. Lett. **59A**, 486 (1977); J. Appl. Phys. **53**, 7927 (1982).
[25] C. Domb, Adv. Phys. **9**, 149 (1960).
[26] P. A. Rikvold, W. Kinzel, J. D. Gunton, and K. Kaski, Phys. Rev. B **28**, 2686 (1983).
[27] B. Derrida and L. deSeze, J. Phys. (Paris) **43**, 475 (1982).
[28] J. L. Cardy, J. Phys. A **17**, L385 (1984).
[29] N. Metropolis, A. W. Rosenbluth, A. H. Teller, and E. Teller, J. Chem. Phys. **21**, 1087 (1953).
[30] J. B. Collins, P. A. Rikvold, and E. T. Gawlinski, Phys. Rev. B **38**, 6741 (1988).
[31] H. E. Stanley, *Introduction to Phase Transitions and Critical Phenomena* (Oxford University Press, Oxford, 1971).
[32] B. M. McCoy and T. T. Wu, *The Two-dimensional Ising Model* (Harvard University Press, Cambridge, MA, 1973).
[33] M. P. M. den Nijs, J. Phys. A **12**, 1857 (1979).
[34] B. Nienhuis, E. K. Riedel, and M. Schick, J. Phys. A **13**, L189 (1980).